Composite Interfaces, 2013
Vol. 20, No. 6, 395–404, http://dx.doi.org/10.1080/15685543.2013.807145

On the toughness of thermoplastic polymer nanocomposites as assessed by the essential work of fracture (EWF) approach

J. Karger-Kocsis[a,b]*, V.M. Khumalo[c], T. Bárány[b], L. Mészáros[b] and A. Pegoretti[d]

[a]*MTA–BME Research Group for Composite Science and Technology, Műegyetem rkp. 3, Budapest H-1111, Hungary;* [b]*Department of Polymer Engineering, Faculty of Mechanical Engineering, Budapest University of Technology and Economics, Műegyetem rkp. 3, Budapest H-1111, Hungary;* [c]*Department of Polymer Technology, Faculty of Mechanical Engineering and Built Environment, Tshwane University of Technology, Pretoria 0001, South Africa;* [d]*Department of Materials Engineering and Industrial Technologies, University of Trento, Trento I-38123, Italy*

(*Received 27 February 2013; accepted 25 April 2013*)

The essential work of fracture (EWF) approach is widely used to determine the plane stress fracture toughness of highly ductile polymers and related systems. To shed light on how the toughness is affected by nanofillers EWF-suited model polymers, viz. amorphous copolyester and polypropylene block copolymer were modified by multiwall carbon nanotube (MWCNT), graphene (GR), boehmite alumina (BA), and organoclay (MMT) in 1 wt% each. EWF tests were performed on deeply double-edge notched tensile-loaded specimens under quasistatic loading conditions. Data reduction occurred by energy partitioning between yielding and necking/tearing. The EWF prerequisites were not met with the nanocomposites containing MWCNT and GR by contrast to those with MMT and BA. Accordingly, the toughness of nanocomposites with homogeneously dispersed and low aspect ratio fillers may be properly determined using the EWF. Results indicated that incorporation of nanofillers may result in an adverse effect between the specific essential and non-essential EWF parameters.

Keywords: toughness; nanocomposite; thermoplastics; essential work of fracture

1. Introduction

The essential work of fracture (EWF) concept became very popular to characterize the plane stress toughness of ductile polymers and related systems. The widespread use of the EWF is due to the simple specimens' preparation, easy testing, and simple data reduction procedure. Though the EWF method is dominantly used for mode-I type loading, it has been successfully adopted for mode-II and mode-III type deformations, too. Moreover, attempts were also made to deduce plane strain toughness values from EWF tests.[1]

According to the EWF, the total work of fracture (W_f) can be partitioned into two components: (i) the EWF (W_e) consumed in the inner fracture process zone to create new surface and (ii) the nonessential (or plastic) work (W_p) performed in the outer 'plastic' deformation zone. The related zones, being surface- and volume-related,

*Corresponding author. Email: karger@pt.bme.hu

respectively, are shown schematically in case of a deeply double-edge notched tensile-loaded (DEN-T) specimen in Figure 1.

The total work of fracture (W_f), calculated from the area of the force-displacement (F-x) curves, is given by:

$$W_f = W_e + W_p \tag{1}$$

Equation (1) can be rewritten into the specific terms (Equations (2) and (3)):

$$W_f = w_e \times Lt + \beta w_p \times L^2 t \tag{2}$$

$$w_f = w_e + \beta w_p \times L \tag{3}$$

where L is the ligament length, t is the specimen thickness, and β is the shape factor related to the form of the outer plastic dissipation zone. Equation (3) is the base of data reduction: the specific work of fracture data is determined on specimens with varying ligaments are plotted as a function of the ligament length. w_e is given by the $y(w_f)$-intercept of the linear regression fitted on the w_f vs. L data. Its value can be equalled with the resistance to crack initiation. The slope (βw_p) of the linear regression can be treated as a measure of the resistance to the crack growth of the material. Detailed information on the EWF testing, data reduction, and interpretation can be taken from recent reviews.[1,2]

The easy performance of the EWF test guided researchers to adapt this technique also for systems where it does not work. This happened also in the past when using the EWF for thermoplastic nanocomposites.[1,3] As a consequence, the published results scatter and do not allow us to make any useful conclusion in respect to the structure–toughness relationships in thermoplastic nanocomposites. This is the right place to mention that according to our terminology nanocomposites contain inorganic or organic additives the size of which, when individually dispersed, is less than 10 nm at least in

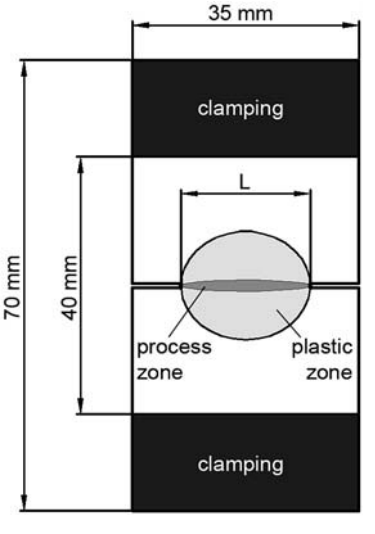

Figure 1. Schematic diagram showing the process and plastic zones in a DEN-T specimen. Designations: L – ligament.

one direction. As a consequence, the term nanocomposite is used also for those systems which contain large agglomerates (submicron or even micron scaled) composed of the above-defined nanofillers.

This work was aimed at studying how the type and dispersion state of various nanofillers affect the toughness of nanocomposites, whereby following the research philosophy: (a) using nanofillers of different aspect ratio and with different dispersibility in polymer melts and (b) choosing such model polymers which satisfy all the requirements of the EWF use. Accordingly, the following fillers were selected: fibrous multiwall carbon nanotube (MWCNT), platy-type graphene (GR) and organophilic-modified montmorillonite (MMT), and quasispherical synthetic boehmite alumina (BA). Unlike MWCNT and GR, hold tightly together by Van der Waals forces, MMT,[4] and especially BA [5–7] can be adequately dispersed in various thermoplastics via melt compounding.

2. Materials and testing methods

2.1. Materials and specimen preparation

As matrix materials poly(propylene-*block*-ethylene) (EPBC; Tipplen K499, TVK Nyrt, Tiszaújváros, Hungary) and poly(ethylene terephthalate glycol) (PETG; Eastar Copolyester 6763, Eastman Chemical Company, Kingsport, TN, USA) were selected. These polymers fulfill the most important EWF requirement, namely full ligament yielding prior to crack growth.[8,9] The selected nanofillers were: MWCNT (Baytubes C 150P; Bayer MaterialScience AG, Leverkusen, Germany), GR (xGnP, XG Sciences Inc., Lansing MI, USA), MMT (Cloisite 30B, Southern Clay Products, Inc., Austin TX, USA), and BA (Disperal P3; Sasol GmbH, Hamburg, Germany). MWCNT was nonfunctionalized with the following characteristics: carbon purity > 95%, number of walls: 3–15, outer diameter range: 5–20 nm, length range: 1–10 μm. Basic properties of GR were: H-grade, approximate thickness of layer stacks: 15 nm, specific surface: 50–80 m^2/g. MMT was an organophilic modified (alkyl quaternary ammonium salt) bentonite with an individual layer thickness of about 1 nm and interlayer spacing: 1.85 nm. Characteristics of BA were: primary crystallite size 4.5 nm, dispersed particle size in water at about 15 nm, specific surface area at about 300 m^2/g. All these fillers were introduced in 1 wt% in the thermoplastics during extrusion melt compounding in a Labtech Scientific type twin-screw extruder ($L/D = 44$; $D = 26$ mm). The granulated nanocomposites were sheeted to a thickness of ca. 0.6 mm by compression molding (Collin Teach-Line Platen Press 200E). During processing the recommendations of the suppliers were followed.

2.2. Testing methods

DEN-T specimens with the dimension 35 × 70 mm (width × length, cf. Figure 1) were subjected to quasistatic loading at 2 mm/min deformation rate at room temperature with a universal testing machine (Zwick Z005, Ulm, Germany). The ligament range covered $L = 5$ to 25 mm. At each ligament five specimens were tested. During the data reduction, the energy partitioning method recommended by Karger–Kocsis [1,9] was adapted:

$$w_f = w_{f,y} + w_{f,n} = \left(w_{e,y} + \beta' w_{p,y} \times L\right) + \left(w_{e,n} + \beta'' w_{p,n} \times L\right) \quad (4)$$

where *y* and *n* subscripts denote the yield- and necking/tearing-related terms.

When the yielding and necking/tearing sections are not well separated, they were differentiated from one another by considering the maximum force.

$$w_f = w_{f,b} + w_{f,n} = \left(w_{e,b} + \beta' w_{p,b} \times L\right) + \left(w_{e,n} + \beta'' w_{p,n} \times L\right) \quad (5)$$

where *b* subscript denotes the blunting-related term.

The failure mode of the specimens was inspected in light (LM; Olympus BX51, Hamburg, Germany) and scanning electron microscopes (SEM; JEOL JSM-6380LA, Tokyo, Japan). The conductivity of the test specimens was ensured by coating with an Au/Pd alloy.

3. Results and discussion

3.1. Force-elongation (F-x) curves and related EWF parameters

Modification with GR and MWCNT strongly affected the *F-x* curves of both PETG and EPBC. Though for the yielding section the self-similarity criterion (i.e. linear transformation results in overlapping of the related curves) fairly holds, this is not at all the case for the necking/tearing part – cf. Figure 2. Accordingly, the w_f vs. L regressions underlayed a large scatter and the related slopes were close to horizontal (i.e. 0) – cf. Figure 3. The correlation coefficients of the linear regressions (R^2) were unacceptably low, as well – cf. Tables 1 and 2. Therefore, the EWF conditions were clearly violated when testing GR and MWCNT modified EPBC and PETG nanocomposites. On the other hand, the EWF approach can still be adapted for their yielding-related loading parts of the corresponding *F-x* curves – cf. Equation (4).

By contrast, the EWF could well be applied for the nanocomposites containing BA and MMT. Figure 4 shows that the *F-x* curves are self-similar. Moreover, the load drop associated with full ligament yielding [1,9] was also well resolved. This was most helpful to perform the energy partitioning according to Equation (4) – cf. Figure 5.

Note that the load drop is prominent for the PETG (cf. Figure 4) but hardly resolvable for EPBC-based BA and MMT nanocomposites (cf. Figure 6). In the case of EPBC, instead of instantaneous yielding a delayed yielding occurred which is termed as

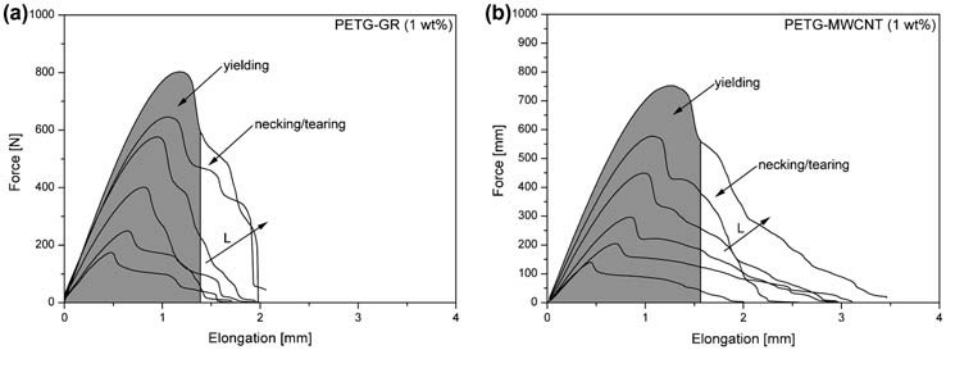

Figure 2. Force-elongation traces as a function of the ligament length (L) measured on DEN-T specimens of PETG-GR (a) and PETG-MWCNT (b). Partitioning between yielding- and necking/tearing-related sections are indicated for the largest ligament specimen.

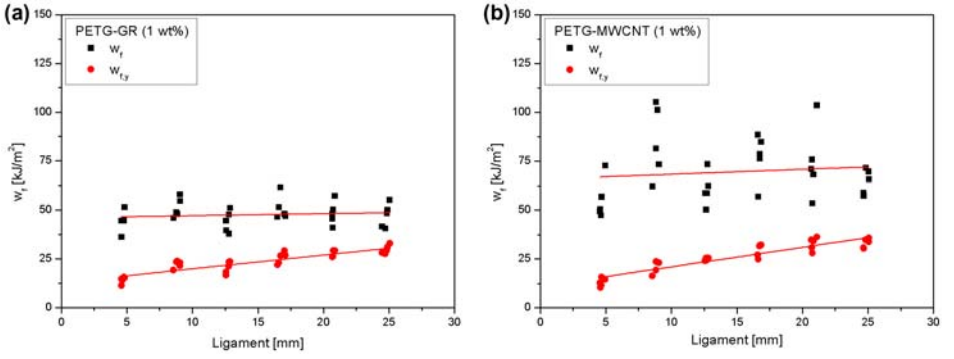

Figure 3. w_f and $w_{f,y}$ vs. ligament traces as a function of the ligament length measured on DEN-T specimens of PETG-GR (a) and PETG-MWCNT (b).

Table 1. Specific essential (w_e) and non-essential (β_{wp}) work of fracture parameters along with those related to blunting ($w_{e,b}$ and $\beta' w_{p,b}$) for the EPBC-based nanocomposites.

	EPBC					
	w_e [kJ/m^2]	βw_p [MJ/m^3]	R^2 [–]	$w_{e,b}$ [kJ/m^2]	$\beta' w_{p,b}$ [MJ/m^3]	R^2 [–]
Matrix	48.3	6.1	0.91	2.8	0.92	0.93
BA	45.0	4.8	0.84	2.7	0.90	0.94
GR	27.6	1.3	0.45	5.4	0.62	0.67
MMT	42.4	5.6	0.87	4.2	0.80	0.85
MWCNT	43.2	0.8	0.20	6.7	0.66	0.73

Note: Blunting was traced to the maximum load of each specimen.

Table 2. Specific essential (w_e) and non-essential (βw_p) work of fracture parameters along with those related to yielding ($w_{e,y}$ and $\beta' w_{p,y}$) for the PETG-based nanocomposites.

	PETG					
	w_e [kJ/m^2]	βw_p [MJ/m^3]	R^2 [–]	$w_{e,y}$ [kJ/m^2]	$\beta' w_{p,y}$ [MJ/m^3]	R^2 [–]
Matrix	56.9	8.3	0.96	15.5	0.92	0.87
BA	51.6	8.3	0.97	9.2	1.12	0.93
GR	46.1	0.1	0.02	12.8	0.71	0.77
MMT	33.8	9.7	0.97	7.3	1.25	0.94
MWCNT	65.8	0.2	0.02	11.0	1.00	0.83

blunting.[1,10] Further, premature failure in the necking/tearing stage often occurred, especially at high L values – cf. Figure 6(a). Nevertheless, the related w_f and $w_{f,b}$ vs. L traces proved to be fairly linear (cf. Figure 7) with rather high R^2 values – cf. Table 1.

Results in Tables 1 and 2 suggest that BA nanofiller only slightly affected the specific EWF parameters. This can be traced to the fact that BA does not influence the morphology of either amorphous or semicrystalline polymers markedly.[5,6,11] The scenario is somewhat different for MMT which is prone for the formations intercalated tactoids and may have a large impact on the morphology of semicrystalline systems.[4]

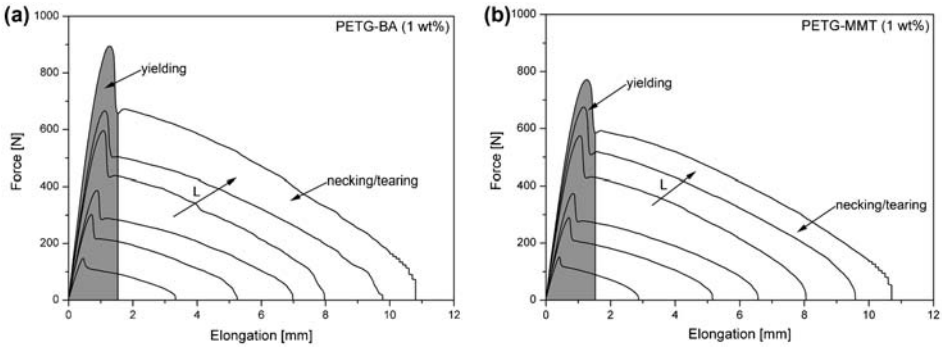

Figure 4. Force-elongation traces as a function of the ligament length (L) measured on DEN-T specimens of PETG-BA (a) and PETG-MMT nanocomposites (b). Partitioning between yielding- and necking/tearing-related sections are indicated for the largest ligament specimen.

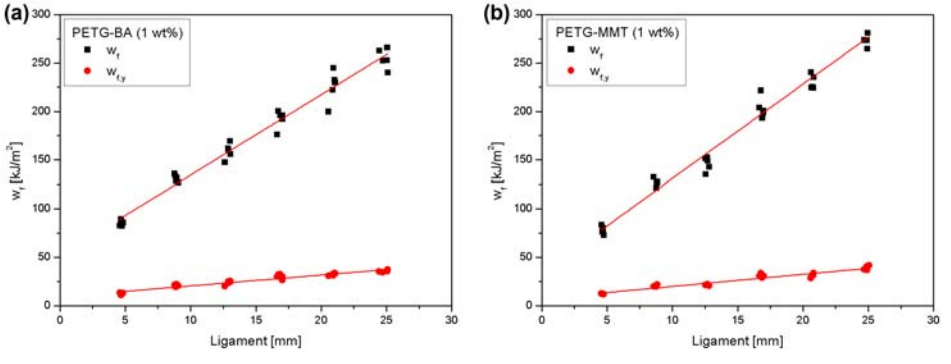

Figure 5. w_f and $w_{f,y}$ vs. ligament traces as a function of the ligament length (L) measured on DEN-T specimens of PETG-BA (a) and PETG-MMT (b).

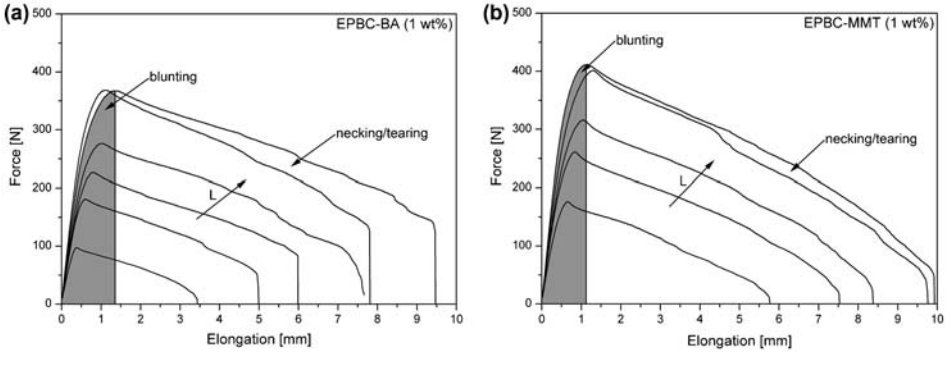

Figure 6. Force-elongation traces as a function of the ligament length (L) measured on DEN-T specimens of EPBC-BA (a) and EPBC-MMT nanocomposites (b). Partitioning between blunting- and necking/tearing-related sections are indicated for the largest ligament specimen.

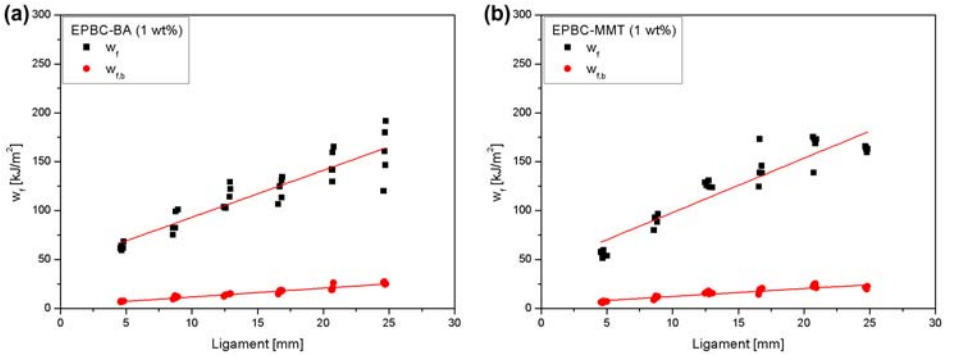

Figure 7. w_f and $w_{f,b}$ vs. ligament traces measured on DEN-T specimens of EPBC-BA (a) and EPBC-MMT (b).
Note: $w_{f,b}$ is the blunting-related specific work of fracture calculated by considering the absorbed energy until the maximum load.

This may be the reason for the different changes in the yielding-related terms, i.e. $w_{e,b}$ was enhanced and $\beta' w_{p,b}$ reduced for EPBC/MMT, whereas $w_{e,y}$ was reduced and $\beta' w_{p,y}$ slightly enhanced for PETG/MMT.

3.2. *Failure*

LM pictures were taken from the plastic zone areas of the DEN-T specimens of the neat and modified PETG (cf. Figure 8). One can see that the plastic zone is well developed and of elliptical shape for the unmodified, BA- and MMT-filled systems. By contrast, this is not the case for the GR-containing PETG. Though the latter specimen experienced full ligament yielding, the necking/tearing stage became instable due to the inhomogeneous dispersion of the relatively large amount of GR, which in addition has a high aspect ratio. It is noteworthy that unstable fracture in the necking/tearing stage is usually triggered by increasing deformation rate or decreasing molecular weight in unfilled polymers.[1]

SEM picture taken of the transition zone from the bulk toward the plastic zone of PETG-BA (cf. Figure 9(a)) indicates that the latter was generated by shear yielding. In the plastic zone, some BA-induced voiding can be resolved owing to larger agglomerates. The gross yielding of PETG is, however, not influenced even by larger agglomerates of BA. Figure 9(b) supports that BA particles can be treated as quasi-spherical ones, in fact.

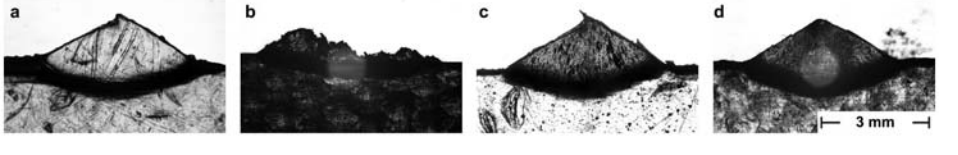

Figure 8. LM pictures taken from the failed DEN-T specimens of the neat PETG (a), and its nanocomposites containing GR (b), BA (c) and MMT (d), respectively.

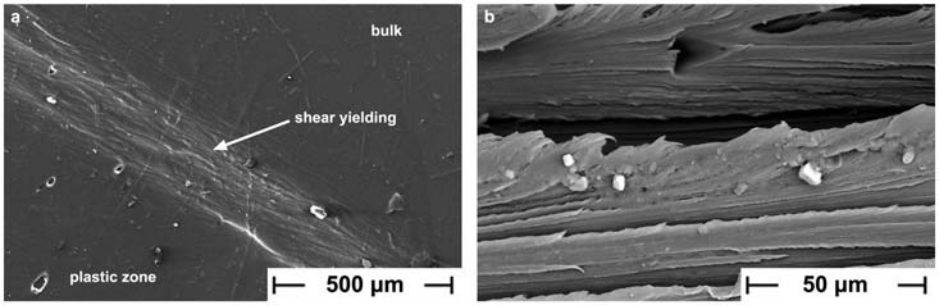

Figure 9. SEM pictures from the surface of the transition between the plastic zone and bulk (a) and from the fracture zone (b) of a DEN-T specimen of PETG-BA.
Note: Picture (b) shows micron-scaled agglomerates.

Similar to PETG-BA, the smooth development of the plastic zone in PETG-MMT should be ascribed to the homogeneous distribution of the MMT tactoids (not reported here) which thus have markedly smaller aspect ratios than GR or MWCNT.

The development of the plastic zone and the corresponding failure mode of the EPBC nanocomposites were more complex than those of the PETG-based ones due to the onset of massive crazing. The latter resulted in a 'stress-whitened' plastic zone. Nonetheless, the overall appearance of the plastic zone of the EPBC systems was very similar to those of the PETG-based ones – cf. LM frames in Figure 8. Figure 10 compares the fracture surfaces (i.e. process zones) of the DENT-specimens with BA, MMT, MWCNT, and GR nanofillers. All nanocomposites failed ductilely via voiding/crazing, followed by void/craze growth with extensive fibrillation.[12] Voiding is caused by the

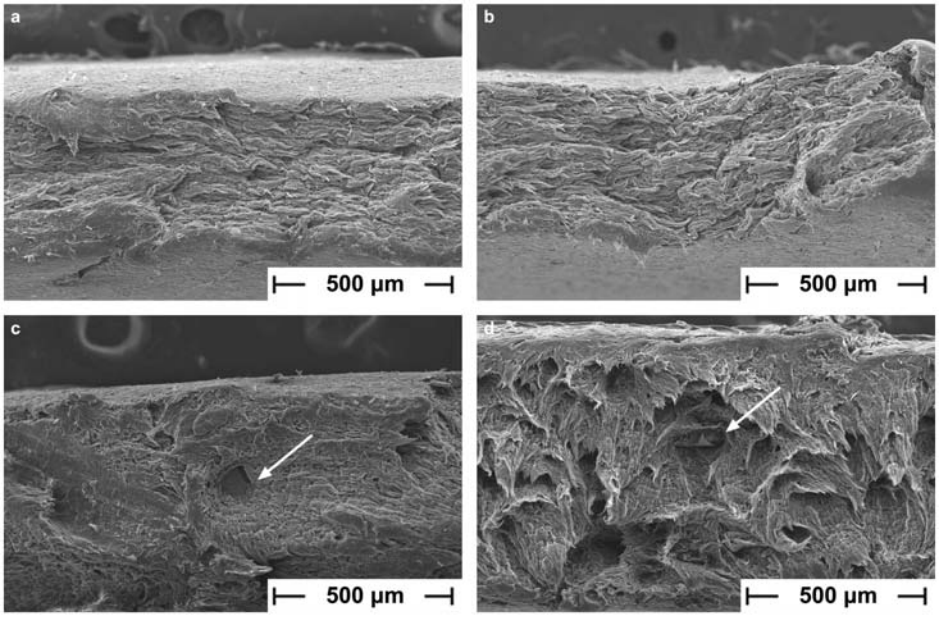

Figure 10. SEM pictures from the fracture zones of DEN-T specimens of EPBC-BA (a), EPBC-MMT (b), EPBC-GR (c), and EPBC-MWCNT (d).
Note: secondary cracking is indicated by arrows.

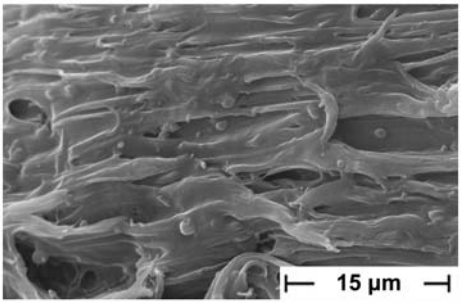

Figure 11. SEM picture from the fracture zone of EPBC-BA.

filler particles, acting as stress concentrators, and easily detaching from the matrix. The difference in the failure between the nanocomposites is due to the fillers' dispersion. The ductile deformation of the EPBC is less influenced by the homogeneously and finely dispersed fillers, like BA (cf. Figure 11). It is noteworthy that the dispersed BA particles, being in submicron range, are large agglomerates when considering the primary particle size of BA, namely 4.5 nm. Recall that BA was dispersed in agglomerated form even in water (mean particle size of the 10 wt% BA containing aqueous dispersion was at about 15 nm according to the manufacturer's leaflet). By contrast, large agglomerates, like GR and MWCNT in Figure 10(c) and (d), induce secondary cracking and results in a highly inhomogeneous stress field. This hampers the craze growth with fibrillation, the final outcome of which is a premature failure. This is the reason why the DEN-T specimens failed by instable necking/tearing. This manifested in unreliable EWF data – cf. Table 1.

4. Conclusion

The EWF concept has limited applicability for thermoplastic nanocomposites, even when such polymers are selected as matrices which in unmodified form meet all the necessary requirements, such as the chosen PETG and EPBC. Nanofillers, present in inhomogeneous distribution and possessing large aspect ratio, trigger unstable fracture in the necking/tearing stage. This is due to an inhomogeneous stress field created which hampers the full development of shear yielding (PETG) and voiding/crazing (EPBC). As a consequence, the traditional EWF data reduction becomes inapplicable. This problem can be overcome in some cases by the energy partitioning provided that for the yielding section of the load–displacement traces the self-similarity criterion holds. The toughness of nanocomposites with homogeneously dispersed and low aspect ratio fillers may be properly determined using the EWF. On the other hand, further investigations are needed to check how the EWF parameters are affected by the nanofillers' inherent (composition, aspect ratio, surface coating, etc.) and dispersion characteristics in the matrices.

Acknowledgements

This work was performed in the framework of a bilateral cooperation agreement between Italy and Hungary (TéT_10-1-2011-0218). This work is connected to the scientific program of the 'Development of quality-oriented and harmonized R+D+I strategy and functional model at BME' and to the New Széchenyi Plan (Projects IDs: TÁMOP-4.2.1/B-09/1/KMR-2010-0002, TÁMOP-4.2.2.B-10/1-2010-0009 and TÁMOP 4.2.4. A/1-11-1-2012-0001).

References

[1] Bárány T, Czigány T, Karger-Kocsis J. Application of the essential work of fracture (EWF) concept for polymers, related blends and composites. Progr. Polym. Sci. 2010;35:1257–1287.
[2] Martinez AB, Gamez-Perez J, Sanchez-Soto M, Velasco JI, Santana OO. Maspoch MLl. The essential work of fracture (EWF) method – analyzing the post-yielding fracture mechanics of polymers. Eng. Fract. Mech. 2009;16:2604–2617.
[3] Karger-Kocsis J. Chapter 12: On the toughness of "nanomodified" polymers and their traditional polymer composites. In: Karger-Kocsis J, Fakirov S, editors. Nano- and micromechanics of polymer blends and composites. Munich: Hanser; 2009. p. 426–470.
[4] Utracki LA. Clay-containing polymeric nanocomposites. Shawbury: Rapra Technology; 2004.
[5] Streller RC, Thomann R, Torno O, Mülhaupt R. Morphology, crystallization behavior, and mechanical properties of isotactic poly(propylene) nanocomposites based on organophilic boehmite. Macromol. Mater. Eng. 2009;294:380–388.
[6] Ogunniran ES, Sadiku R, Sinha Ray S, Luruli Ny. Morphology and thermal properties of compatibilized PA12/PP blends with boehmite alumina nanofillers inclusions. Macromol. Mater. Eng. 2012;297:627–638.
[7] Pedrazzoli D, Ceccato R, Karger-Kocsis J, Pegoretti A. Viscoelastic behaviour and fracture toughness of linear-low-density polyethylene reinforced with synthetic boehmite alumina nanoparticles. Express Polym. Lett. 2013;7:652–666.
[8] Maspoch MLl, Gámez-Perez J, Gordillo A, Sánchez-Soto M, Velasco JI. Characterization of injected EPBC plaques using the essential work of fracture (EWF) method. Polymer. 2002;43:4177–4183.
[9] Karger-Kocsis J. For what kind of polymer is the toughness assessment by the essential work concept straightforward? Polym. Bull. 1996;37:119–126.
[10] Karger-Kocsis J, Bárány T. Plane-stress fracture behavior of syndiotactic polypropylenes of various crystallinity as assessed by the essential work of fracture method. Polym. Eng. Sci. 2002;42:1410–1419.
[11] Tuba T, Khumalo VM, Karger-Kocsis J. Essential work of fracture of poly(ε-caprolactone)/boehmite aluminananocomposites: effect of surface coating. J. Appl. Polym. Sci. 2013;129:2950–2958. doi:10.1002/app.39004
[12] Michler GH, Baltá-Calleja FJ. Nano- and micromechanics of polymers. Munich: Hanser; 2012.